Nonlinear deep-water waves: theory and experiment. Part 2. Evolution of a continuous wave train

By BRUCE M. LAKE, HENRY C. YUEN, HARALD RUNGALDIER AND WARREN E. FERGUSON†

Fluid Mechanics Department, TRW/DSSG, One Space Park, Redondo Beach, California 90278

Results of an experimental investigation of the evolution of a nonlinear wave train on deep water are reported. The initial stage of evolution is found to be characterized by exponential growth of a modulational instability, as was first discovered by Benjamin & Feir. At later stages of evolution it is found that the instability does not lead to wave-train disintegration or loss of coherence. Instead, the modulation periodically increases and decreases, and the wave train exhibits the Fermi–Pasta–Ulam recurrence phenomenon. Results of an earlier study of nonlinear wave packets by Yuen & Lake, in which solutions of the nonlinear Schrödinger equation were shown to provide quantitatively correct descriptions of the properties of nonlinear wave packets, are applied to describe the experimentally observed wave-train phenomena. A comparison between the laboratory data and numerical solutions of the nonlinear Schrödinger equation for the long-time evolution of nonlinear wave trains is given.

1. Introduction

One of the first detailed investigations of the time evolution of nonlinear deep-water waves was performed by Lighthill (1965), who examined the evolution of a smooth initial wave packet using the averaged Lagrangian theory developed by Whitham (1965). His solution predicted that the nonlinearity would lead to a focusing of energy towards the centre of the pulse as the packet evolved in time, but the solution became singular within a finite time. Lighthill commented that such behaviour is indicative of the presence of an instability associated with nonlinear deep-water waves. Two years later, Benjamin & Feir (1967), using a perturbation approach, demonstrated that a uniform continuous wave train is unstable to modulational perturbations of its envelope. The same problem was examined by Lighthill (1967) using Whitham's theory. While both results predict instability, they differ in the details of the conditions for instability. Neither of the results yields any information regarding the long-time behaviour of the wave train. The Benjamin & Feir results are limited to the initial instability, while Lighthill's solution again leads to a singularity in a finite time, as in the case of wave packets, although in principle Whitham's theory should be asymptotically valid.

† Permanent address: Department of Mathematics, University of Arizona, Tucson, Arizona 85712.

Further progress in the subject was made by Chu & Mei (1970, 1971), who used a multi-scale method to derive the governing equations. Their equations are similar to those used by Lighthill (1965) except for an additional term in the dispersion relation, which was shown to be of the same order as the nonlinear correction. The presence of this term, a term proportional to $a^{-1} \partial^2 a / \partial x^2$, where a is the amplitude of the wave envelope, changes the mathematical nature of the equations and eliminates the singularity encountered by Lighthill (1965, 1967). However, because of the appearance of a in the denominator, their numerical calculations are also limited to a finite time since the computation breaks down whenever a vanishes at any point.

Zakharov (1968) (and later Hasimoto & Ono 1972; Davey 1972) showed that, if the wavenumber variation is small, the governing equations can be reduced to a single equation for the complex wave envelope: the nonlinear Schrödinger equation. Later, Zakharov & Shabat (1972) solved exactly the initial-value problem for the nonlinear Schrödinger equation for initial conditions which decay to zero sufficiently rapidly. The exact solutions predict that an arbitrary smooth initial wave packet will eventually disintegrate into a definite number of permanent wave packets (envelope solitons) which are stable to collisions. Yuen & Lake (1975) then proved that Whitham's theory, when applied consistently to the order considered, yields the same nonlinear Schrödinger equation. With this finding, the apparent discrepancies between Whitham's theory and the results of Benjamin & Feir are resolved, since the nonlinear Schrödinger equation reproduces the Benjamin & Feir instability for the case of an initially uniform nonlinear wave train.

Despite the interest in the subject, surprisingly few experimental results have been published. Benjamin & Feir (1967) and Benjamin (1967) have presented some experimental evidence which qualitatively supports their analysis. Feir (1967) also exhibited some results on the evolution of an initial wave packet, which were later used by Chu & Mei to obtain comparisons between experimental measurements and the results of their numerical calculations. A systematic testing of the quantitative aspect of the theory by well-controlled experiments was not undertaken until 1975, when Yuen & Lake (1975) verified that the nonlinear Schrödinger equation provides a quantitatively satisfactory description of the long-time evolution of wave packets. Lake & Yuen (1977) then re-examined the experiments on the initial instability of wave trains and accounted for the apparent discrepancies that existed between the analytical and experimental results of Benjamin and Feir as they presented them (Benjamin & Feir 1967; Benjamin 1967).

Despite the encouraging agreement between experiment and theory for the long-time evolution of nonlinear wave-envelope pulses and for the initial instability of nonlinear continuous wave trains, there has not been a consensus of opinion regarding the long-time behaviour of a continuous wave train. As discussed in §3.2 of this paper, theoretical arguments have been used by Benjamin, Hasselmann, Chu & Mei and others to propose several possible, and mutually exclusive, end states of wave-train evolution. Because experimental evidence of the kind which might serve to identify the correct long-time behaviour was not available, we began an experimental investigation of the evolution of nonlinear continuous wave trains. In this paper we report the results of that experimental investigation, in which we have studied wave-train evolution from the initial onset of instability on uniform or nearly uniform wave trains to the long-time behaviour of the wave trains during and after the stage where

the resulting amplitude modulations become very strong. The experimental results are then considered as they relate to the known properties of nonlinear wave pulses and the results of numerical solutions of the nonlinear Schrödinger equation for the evolution of continuous wave trains. We believe that the results of these investigations reveal the correct long-time behaviour of nonlinear continuous wave trains on deep water.

2. Experiment

The experiments were performed in a $3 \times 3 \times 40$ ft water tank. A programmable surface wave maker is located at one end of the tank and a simple but effective (reflected amplitude/incident amplitude $\leqslant 5\%$) wave-absorbing beach at the opposite end. The evolution of surface wave trains was measured as they propagated down the tank from the wave maker to the beach, using capacitance-type wave amplitude gauges located at stations 5, 10, 15, 20, 25 and 30 ft downstream of the wave maker.

The wave maker is a hinged paddle activated by a hydraulic cylinder. The hydraulic system which drives the cylinder is controlled by a servo-amplifier and feedback position transducer, so that the paddle motion is constrained to follow the wave form of the electronic signal applied at the input of the servo-amplifier. The electronic input wave forms are prescribed by computer-generated analog tape recordings. In this way, the particular wave forms of interest could be accurately produced in the wave tank for an amplitude range of 0·01–2·0 in. (peak to peak) and for a frequency range of 1–5 Hz. The wave-maker system is supported on structures that are mounted directly on the laboratory floor and are not on the wave tank itself. In this way, mechanical vibrations associated with operation of the wave-maker system components have been effectively isolated from the wave tank. To keep the distilled water in the facility clean, and to ensure that the dynamics of the surface waves are not subject to effects of surface films, the facility is provided with two 5 μm filtering systems, including a surface skimmer, an ultra-violet sterilizer and a deionizer. The skimmer and plumbing inlets were removed and the filter systems shut down during experiments, so that these systems in no way interfered with fluid motions during the measurements of wave evolution.

The experiments were performed using either purely sinusoidal signals from commercially available function generators or FM tape recordings of computer-generated wave forms as inputs to the wave-maker servo-system. Tape recordings were used whenever wave forms with more than one prescribed frequency component were required. These wave forms were composed of a carrier wave of prescribed frequency f and a pair of side-band frequency components $f \pm \Delta f$ having prescribed values of Δf. The magnitudes of the side-band amplitudes relative to those of the carrier waves were also prescribed. In all the experiments described in this paper, the amplitudes of the prescribed side-band components of any single initial wave form were equal. A wide range of initial wave forms was used, however, in which f, Δf and the ratio $S_0 =$ side-band amplitude/carrier amplitude were varied. The initial wave-form input signals, whether from tape recordings or function generators, were played into the wave-maker servo-system through a variable-gain amplifier which allowed the overall amplitude of the wave form to be controlled. In this way, the amplitudes and slopes of any given initial wave form could be prescribed and set over a wide range of values.

Actual wave amplitude measurements from the gauge at the 5 ft station were used to set particular initial wave amplitudes and slopes. The relationship between the values of ka obtained from measurements of frequency and amplitude at this first downstream station and the initial values of ka used in the theory as the measure of initial non-linearity of Stokes wave trains is discussed in §3.1, and in more detail in Lake & Yuen (1977).

Wave amplitudes were measured using capacitance-type gauges with extremely stable solid-state circuitry and single-element probes made of 0·010 in. o.d. hypodermic tubing. The hypodermic probes provide high resolution measurements of the wave forms (which requires a small probe diameter), while retaining the stiffness required to resist wave-induced motions of the probe itself (which would introduce measurement errors). The wave amplitude gauges were calibrated before and after each series of experiments to assure that measurements were not subject to errors produced by calibration changes. The calibrations were performed using vertical traverse mechanisms mounted above the water surface in the wave tank. The gauge outputs were linearly proportional to wave amplitude, with sensitivities typically 3 V/in. over a 2 in. range. During the experiments, the gauges were supported above the water surface by adjustable struts attached to the top edges of the tank walls so that the sensitive portion of each probe was centred around the mean water level. Although the output of every gauge was linearly proportional to the wave amplitude, each gauge had a slightly different sensitivity. As a result, the oscillograph record of the output voltage from any given probe is an accurate representation of the wave form of the water waves measured by that probe, but the absolute magnitudes of the wave forms shown in oscillograph records recorded by different probes cannot be used to compare actual wave amplitudes at different measurement stations unless differences in probe sensitivity are taken into account. The series of oscillograph records used in several of the figures in this paper are therefore true representations of the wave form changes which occur as wave trains evolve, but should not be used to compare wave amplitudes at different measurement stations.

Typically, experiments were performed by feeding the input signal (from a tape recording or a function generator) for the desired wave form into the wave-maker servo-system and using the wave amplitude measurement at the 5 ft station to adjust the system amplifier gain until the desired initial wave amplitude was obtained. The output signals from the wave amplitude gauges were displayed on a multi-channel oscillograph recorder to monitor the gauge outputs and produce records of the measured wave form. The gauge outputs were also tape recorded, together with an identifying coded time signal, using a fourteen-channel FM tape recorder. Each experimental condition or run was recorded for at least 12 min of real time in order to provide data samples sufficiently long for accurate generation of power spectra. For nearly all of the experiments described in this paper, the quantitative information of primary interest (side-band amplitude levels, side-band growth rates, side-band frequencies, etc.) was obtained from wave amplitude power spectra. The spectra were typically calculated for a frequency range of 0·1–16 Hz, using 16 ensemble averages for a resolution band-width of 0·05 Hz. The range of carrier frequencies used was from 1·5 Hz to 3·5 Hz. The initial values of ka used in these experiments were typically from 0·10 to 0·35, although some cases were run for values as low as 0·03. When experiments were performed using modulated wave forms as inputs to the wave-maker servo-system, the nor-

malized amplitude S_0 of the imposed side-band components was varied from 0·01 to 0·50. Additional details regarding the facilities and procedures used in these experiments may be found in Lewis, Lake & Ko (1974), Yuen & Lake (1975), and Lake *et al.* (1976).

3. Results

3.1. *Initial stage of evolution: the Benjamin–Feir instability*

Benjamin & Feir (1967) have shown that a periodic wave train with initially uniform, finite amplitude is unstable to infinitesimal perturbations in side-band frequency components in the range $0 < \delta \leqslant 2^{\frac{1}{2}}ka$, where k is the wavenumber, a is the wave amplitude and $\delta = \Delta f/f$ measures the frequency separation of the side-band and fundamental components. Their analysis also predicts that the unstable side-band components will grow exponentially at a time rate Ω which depends on δ and ka and is given by $\Omega = \pi\delta(2k^2a^2 - \delta^2)^{\frac{1}{2}}f$, with the maximum growth occurring for $\delta = ka$.

In our experimental study, we have measured properties of nonlinear wave trains as they evolve from conditions of initially uniform amplitude as well as from conditions with imposed initial amplitude modulations. When wave trains were generated with initially uniform amplitudes and initial values of ka greater than or equal to 0·1, we observed the onset and growth of periodic amplitude modulations as the wave trains propagated from the wave maker towards the beach in our 40 ft wave tank.† Examples of the growth of such a modulation, as observed in the measured wave forms and their power spectra at several locations along the length of the tank, are shown in figures 1 and 2. In such cases the wave amplitude modulations, which correspond to pairs of side-band frequency components in the power spectra, develop spontaneously from very small random background perturbations. We find from our experiments that, when a wave train of initially uniform amplitude evolves subject only to low levels of random background perturbations, a single pair of side-band frequency components appears and the continued evolution of the wave train is dominated by only that pair. Such behaviour is consistent with the analysis of Benjamin & Feir, which predicts that a nonlinear wave train is most unstable to perturbations at a particular pair of side-band frequencies, given by $\delta = (ka)_0$. We also find from the experiments, however, that the values of δ obtained from either the measured modulation periods or the side-band frequency components in the spectra are consistently lower than the values of ka obtained from measurements of the amplitudes and frequencies of the wave trains at the initial station, which is located 5 ft from the wave paddle. As discussed in Lake & Yuen (1977), this difference is associated with the fact that finite amplitude waves generated by sinusoidal wave-paddle motions do not have true Stokes wave profiles, for they lack suitable second-harmonic components. Although such waves have the intended amplitude and frequency, they are effectively 'less nonlinear' than amplitude and frequency measurements would indicate. The values of ka obtained from the measurements of the first-order quantities f and a, through use of the formula

$$(ka)_{\mathrm{meas}} = (2\pi f)^2 a/g,$$

† When uniform wave trains with initial values of ka less than 0·1 were generated, measurable amplitude modulations did not develop within our tank length, presumably because of the combined effects of dissipation and the low growth rates of the modulations in such cases.

$x = 5$ ft

$x = 10$ ft
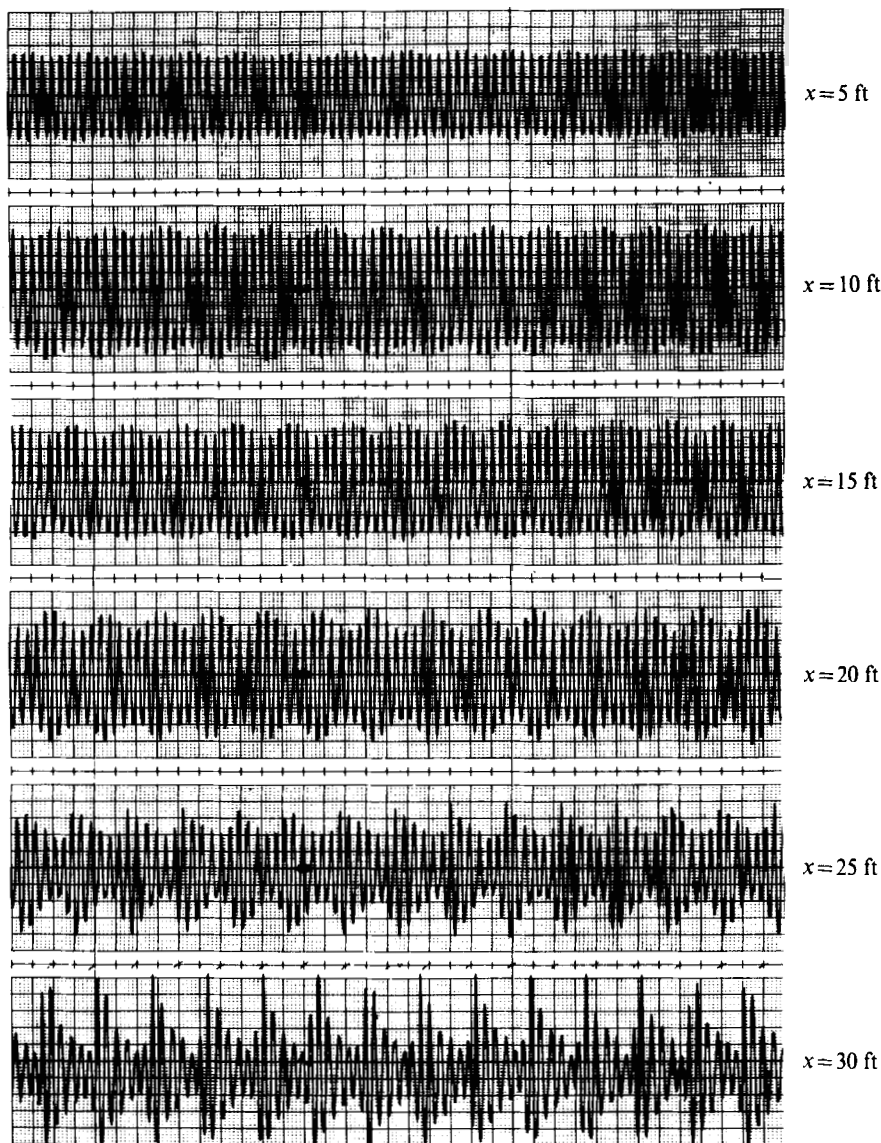
$x = 15$ ft

$x = 20$ ft

$x = 25$ ft

$x = 30$ ft

FIGURE 1. Wave amplitude measurements showing the onset and growth of the Benjamin & Feir modulational instability on an initially unmodulated nonlinear wave train.

produce an overestimate of the nonlinearity of the paddle-generated waves in the experiments when compared with the measure of nonlinearity provided by the second-order quantity ka for Stokes wave profiles in the theory. As a result, a correction factor must be introduced when experimental results are compared with theoretical predictions. Lake & Yuen (1977) have used the Benjamin & Feir prediction that $\delta = (ka)_0$ for the most unstable side-band components, together with measurements of δ for modulations which develop on paddle-generated wave trains of initially uniform amplitude, to obtain a relationship between the values of ka obtained from amplitude and frequency measurements [i.e. $(ka)_{\mathrm{meas}}$] and the values of ka which correctly
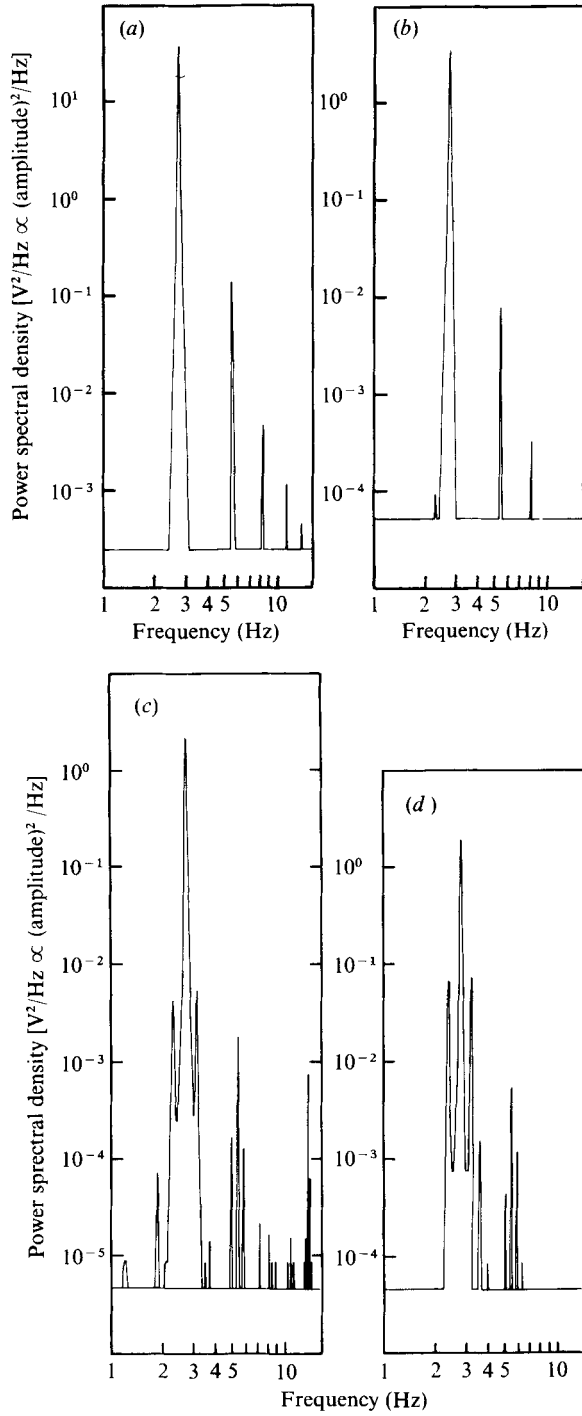
FIGURE 2. Measured wave amplitude spectra showing emergence and growth of the most unstable, $\delta = (ka)_0$, side bands from background noise level. (a) $x = 5$ ft, (b) $x = 10$ ft, (c) $x = 20$ ft, (d) $x = 30$ ft.

characterize the nonlinearity of the wave train for comparison with theory (obtained from the condition that $(ka)_0 = \delta$, using the measured values of δ). They find that $(ka)_0 (= \delta) = 0.78 (ka)_{\text{meas}}$ and, further, that when this correction factor is used good quantitative agreement is obtained between the modulation growth rates predicted by the theory and those measured experimentally, including growth rates measured in experiments where initial modulations were imposed at frequency separations for which $\delta_{\text{imp}} \neq (ka)_0$,† as well as growth rates measured in experiments reported by Benjamin (1967). The same correction has been applied to the experimentally determined initial values of ka reported in this paper to make them compatible with the assumptions of the theory. As shown in § 3.3, we find that when this is done one also obtains quantitative agreement between experimental and theoretical results for the long-time evolution of nonlinear wave trains.

Spectra, such as those shown in figure 2, have been used to provide quantitative measurements of the growth of amplitude modulations on nonlinear wave trains during the initial stage of their evolution. This was done by normalizing the magnitudes of the two side-band components by the magnitude of the carrier-wave frequency component at each measurement station and plotting the ratios against propagation distance. An example of such a result is shown in figure 3. The use of the ratios of side-band magnitudes to carrier magnitudes removes the first-order effect of dissipation, since the dissipation rates for the side-band and carrier components should be nearly identical owing to the small frequency differences between them. It should be possible, therefore, to make useful comparisons between the experimental side-band growth rates and the side-band growth rates predicted by the inviscid analysis of Benjamin & Feir. This assumption appears to be confirmed by comparisons of the measured and predicted growth rates (as in figure 3), which show good agreement between experiment and theory. In making such comparisons, the temporal growth rate in the theory has been transformed to a spatial growth rate using the linear group velocity, as described in § 3.3 and in Benjamin & Feir (1967). The experimental results conform to the predictions of the Benjamin & Feir analysis in that the upper and lower side-band components are of equal magnitude and grow at the predicted exponential rate throughout the stage of evolution for which their normalized magnitudes are small compared with unity. Furthermore, the data show that the exponential rate of side-band growth remains essentially constant, indicating that the second-order effect of dissipation is also unimportant during the initial stage of evolution, since there appears to be no significant weakening of the overall nonlinearity of the system as a result of energy depletion during this stage.

The data in figure 3 were obtained from a series of experiments which were performed using wave trains having equal values of f, ka and δ. Each wave train was generated with an amplitude modulation imposed initially. The only difference between the individual experiments was that each was performed using initial modulations of a different magnitude. The magnitudes of the imposed initial modulations, as measured by the normalized side-band amplitudes, were $S_0 = 0.01$, 0.05, 0.10 and 0.15. We have found that the measured values of the normalized side-band amplitude

† When side bands were imposed initially at values of δ which differed from $(ka)_0$ by more than about 25 %, another pair of side bands at $\delta = (ka)_0$ grew from background perturbations. In such cases, both pairs of side bands (i.e. both modulations) grew but the most unstable pair, at $\delta = (ka)_0$, grew at the faster rate and eventually became dominant (see Lake *et al.* 1976).
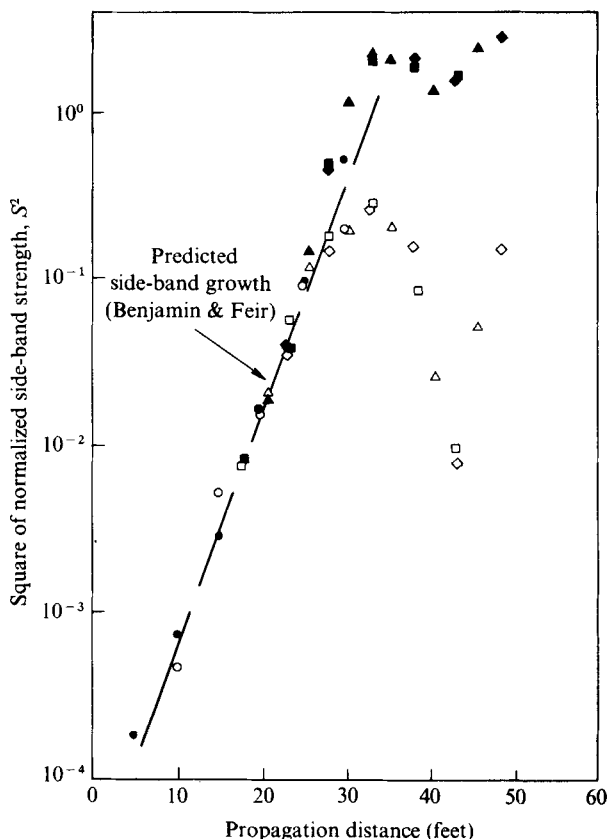
FIGURE 3. Evolution of a nonlinear finite amplitude wave train: normalized side-band amplitudes *vs.* effective propagation distance. Note that the analysis of Benjamin & Feir, which assumes equal side-band amplitudes and predicts the initial side-band growth rate, applies for

$$S^2 < O(10^{-1}).$$

An effective propagation distance that is greater than the tank length has been obtained by performing a series of experiments with progressively higher initial side-band amplitudes. $f_0 = 2 \cdot 5$ Hz, $(ka)_{5\,ft} = \delta = 0 \cdot 2$, $(ka)_0 = 0 \cdot 16$. Solid symbols, lower side band; open symbols, upper side band. Initial side-band amplitude, S_0: $\bigcirc$, 1 %; $\square$, 5 %; $\triangle$, 10 %; $\diamondsuit$, 15 %.

S from such a series of experiments can be plotted against an 'effective' propagation distance in such a way that the data overlap for the entire range of effective propagation distance.† This indicates that the effect of using these different initial side-band amplitudes S_0 is equivalent to re-starting the same experiment at different initial values of the effective propagation distance. In this way, we have been able to measure the characteristics of wave trains as they evolve from nearly unmodulated initial conditions ($S_0 = 0 \cdot 01$) and propagate over distances that are effectively longer than the length of our tank. The results of such experiments, as in figure 3, can be used to

† The data obtained from the experiment performed using initial side-band amplitudes S_0 equal to $0 \cdot 01$ are shown plotted against the actual propagation distance in figure 3. For each set of data obtained from an experiment performed using $S_0 > 0 \cdot 01$, the values of the actual propagation distance were increased by the amount required to place the magnitude of the normalized side-band strength measured at the first probe station on the line defined by the $S_0 = 0 \cdot 01$ data.

identify the stage of wave-train evolution for which the analysis of Benjamin & Feir (a linearized stability analysis which requires that S be small compared with unity) is applicable. They also provide an indication of the characteristics of the long-time evolution of nonlinear wave trains as measured by the normalized amplitudes of the two original side-band components. The data show that the amplitudes of the side-band components are equal and grow at a constant exponential rate until they reach levels such that $S^2 \geqslant O(10^{-1})$. Beyond this stage of evolution the side-band components begin to grow at decreasing rates, and they eventually reach their maximum levels. At the same time, the corresponding spectra show a spread of energy to many modes other than the original three at the side-band and carrier frequencies. Thus the continued evolution of the wave train to still larger effective propagation distances cannot be obtained experimentally using an initial wave form with a single value of S_0 if $S_0^2 > O(10^{-1})$ [as confirmed by experiments using $S_0^2 > O(10^{-1})$], nor can its continued development be described theoretically by an analysis using one pair of side bands and a single value of S. Thus we conclude that for $S^2 > O(10^{-1})$ the Benjamin & Feir analysis is not applicable and further evolution of the wave train must be described by a uniformly valid nonlinear theory.

3.2. *Long-time evolution: FPU recurrence*

The discovery that nonlinear wave trains on deep water are unstable to infinitesimal perturbations of a type which could be expected in any realistic environment led Benjamin & Feir (1967) and Benjamin (1967) to speculate that the resulting exponential growth of amplitude modulations would eventually lead to the disintegration of such wave trains and the redistribution of their energy over a broad spectrum. The possibility that such an end state might be the outcome of the long-time evolution of nonlinear wave trains appears quite plausible in view of the results of the Benjamin & Feir analysis for the initial stage of wave-train evolution. In a discussion of that analysis, however, Hasselmann (1967) went considerably further in statements regarding the implications of the wave-train instability. He interpreted the discovery of the wave-train instability as further evidence for his contention that 'In any wave spectrum, the resonant nonlinear interactions have an irreversible tendency to spread the wave energy evenly over all wavenumbers', a tendency which he had found in an earlier calculation (Hasselmann 1963). We find that this statement, as applied by Hasselmann (1967) to the case of nonlinear wave trains, is directly contradicted by the results of our experimental investigation of the long-time evolution of nonlinear wave trains.† As shown in the following, we find that the resonant nonlinear interactions which lead to the instability of nonlinear wave trains do not have an irreversible tendency to spread energy evenly over all wavenumber components during the long-time evolution of such wave trains.

Chu & Mei (1970, 1971), who studied the nonlinear evolution of the envelope of a deep-water Stokes wave train and found that envelope modulations tend to disinte-

† Although this proposition by Hasselmann has been applied widely in studies of wind waves, results of a recent investigation by Lake & Yuen (1976) indicate that it is also not applicable to the case of nonlinear wind waves. Furthermore, the maintenance of coherence in such nonlinear systems is not confined solely to one-dimensional cases, as has been found by Ferguson & Yuen (1977) in studies of the FPU properties of solutions of the nonlinear Schrödinger equation in two space dimensions.

grate into smaller envelope pulses of permanent form, and Hasimoto & Ono (1972), who discussed the nonlinear Schrödinger equation in the context of nonlinear deep-water waves, have proposed that the end state of the instability of nonlinear wave trains to modulations might be a series of solitary envelope pulses of permanent form. The results of several experimental investigations of nonlinear wave-envelope pulses appear to suggest the possibility of such an end state. Feir (1967) used wave amplitude measurements at two locations in a wave tank to observe the evolution of wave-envelope pulses and reported the first observation of the disintegration of a pulse into more than one pulse. His measurements were performed before the concept of stable envelope pulses or envelope solitons was known, however, and he offered very little explanation of the phenomenon. In a later investigation, Yuen & Lake (1975) reported experimental measurements of the evolution and interaction of wave-envelope pulses which confirm the soliton properties predicted by exact solutions of the nonlinear Schrödinger equation for pulse initial conditions. Their results demonstrate that an arbitrary initial envelope pulse will eventually disintegrate into a number of stable envelope pulses or solitons which have a permanent form as long as dissipative effects are not significant.

In our experimental investigation of nonlinear wave trains, we have observed cases in which initially strongly modulated wave trains have evolved into series of wave-envelope pulses. An example is shown in figure 4. The pulses which develop have profiles that are very similar to both the profiles of the solitons measured in the pulse experiments of Yuen & Lake and the profiles predicted for soliton pulses by solutions of the nonlinear Schrödinger equation. Most of our wave-train experiments indicate, however, that such 'pulse trains' are not the end states of the process of wave-train evolution, and that the wave systems evolve still further.

The series of wave amplitude records shown in figure 5 is more typical of what we have observed in general. During the initial stage of evolution, an initially unmodulated wave train develops an amplitude modulation as predicted by the analysis of Benjamin & Feir (see results for $x = 5$, 10 and 15 ft in figure 5). As the wave train evolves further, the modulation becomes large and the results of their linearized stability analysis no longer apply. Eventually, the modulation becomes so large that where the modulation envelope reaches its minimum levels the amplitudes of individual wave crests approach zero ($x = 25$ ft in figure 5). It is at this stage that wave trains may take on a 'pulse-train' appearance. As the process of evolution continues still further, however, the wave train demodulates and the wave form returns to a relatively uniform state ($x = 30$ ft in figure 5). Experimental results such as these demonstrate that the nonlinear instability of an initially unmodulated wave train does not lead to wave-train disintegration, and that 'pulse trains', if they occur, are simply special strongly modulated stages in a continuing process of wave-train evolution.

Power spectra of wave amplitude measurements at three stages during the evolution of such a wave train are displayed in figure 6. The first shows the spectrum of a wave train during the onset of the initial instability. The carrier-wave frequency, its harmonics and the pair of side-band frequency components corresponding to the growing amplitude modulation are quite evident in the spectrum, even though the wave form itself is still nearly uniform. The second spectrum is one obtained from measurements of the same wave train at a stage where it is undergoing strong modulations, as can be seen in the wave form. At this stage, the wave energy has spread over many frequency
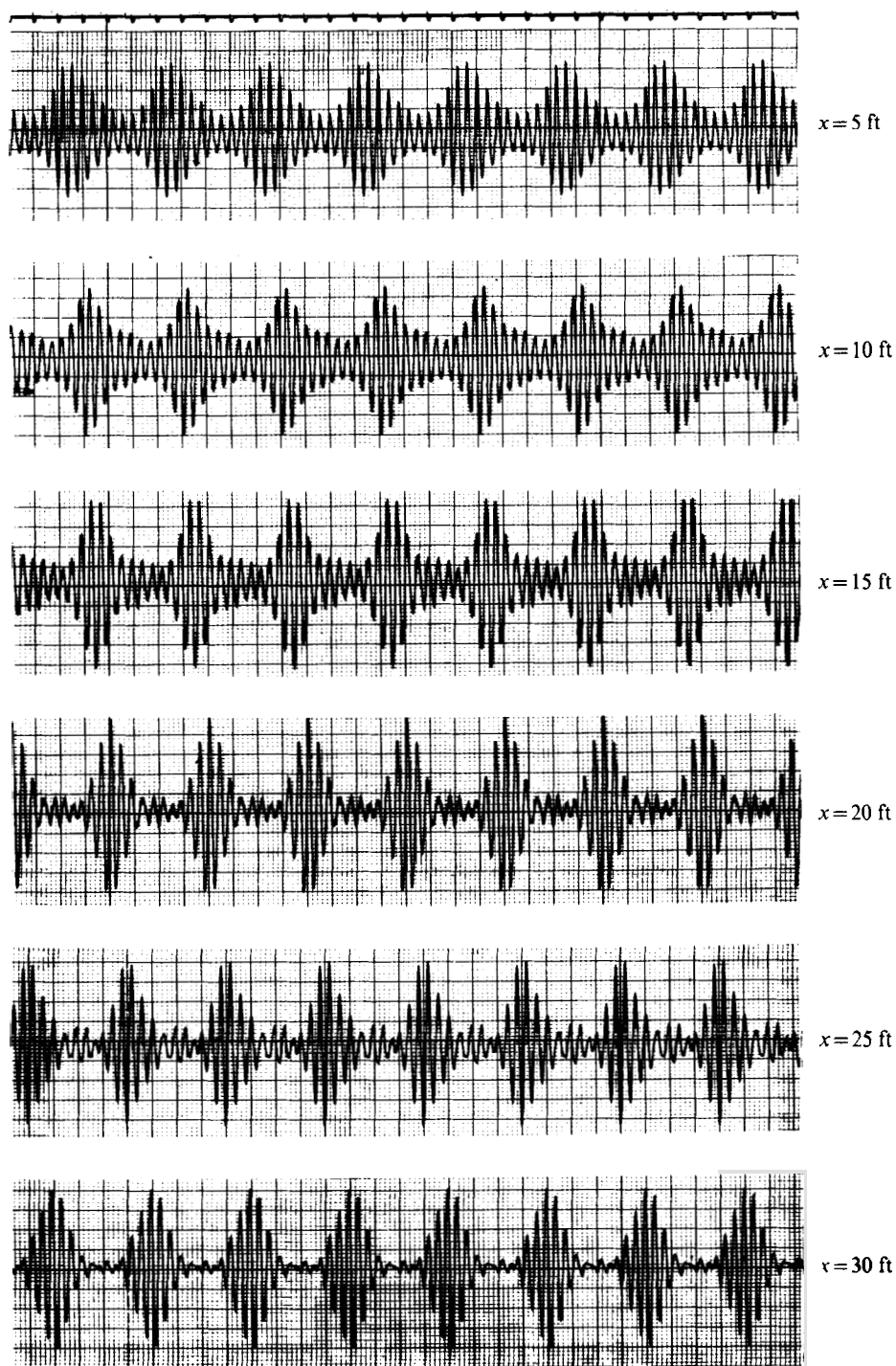
FIGURE 4. Wave amplitude measurements showing the evolution of a modulated wave train into a 'pulse train'. $f_0 = 2\cdot5$ Hz, $(ka)_0 = \delta = 0\cdot1$, $S_0 = 0\cdot5$.
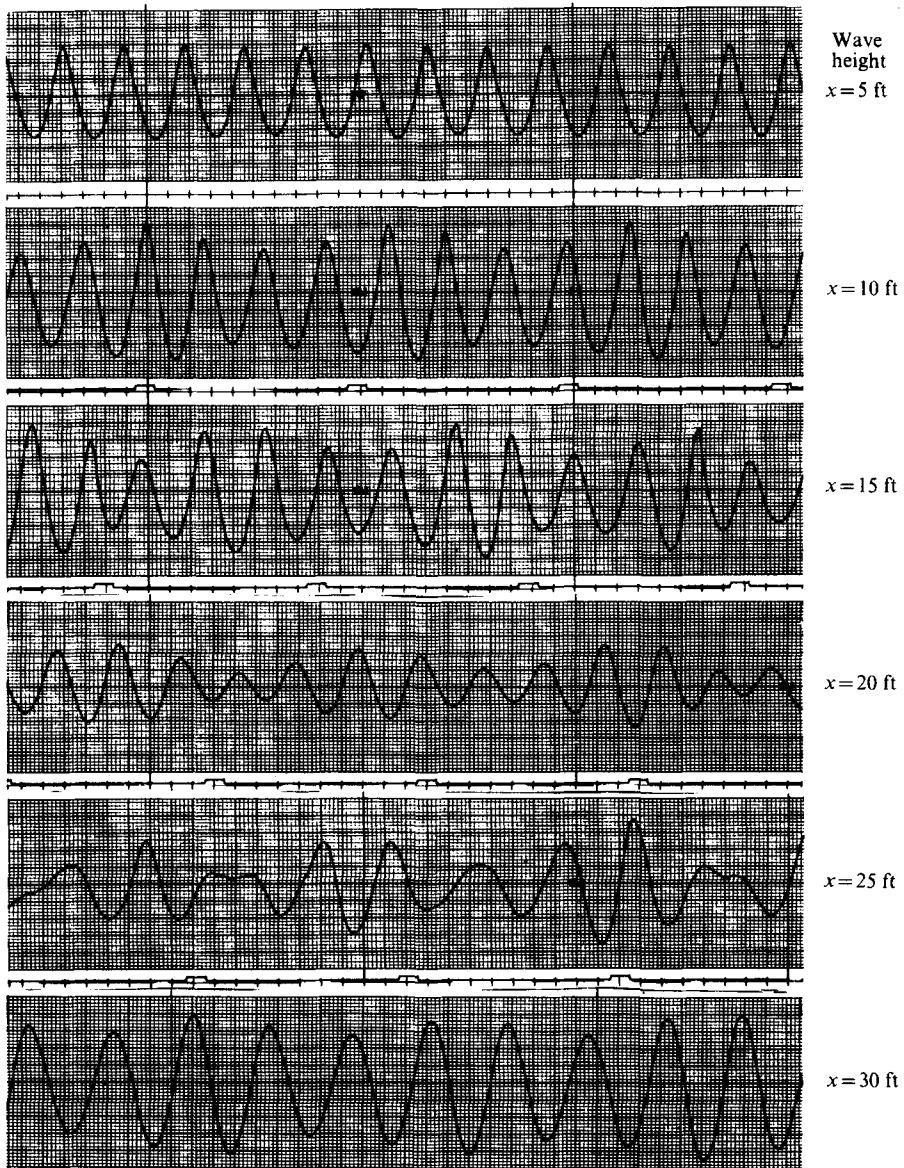
FIGURE 5. Example of the long-time evolution of an initially uniform nonlinear wave train. Initial wave frequency is 3·6 Hz; oscillograph records shown on expanded time scale to display individual wave shapes; wave shapes are not exact repetitions each modulation period because modulation period does not contain integral number of waves.

components in the spectrum. The wave train appears to be in the process of losing its coherence and disintegrating. At a still later stage, however, as shown in the third spectrum, the energy has returned to the original frequency components (carrier, harmonics and side bands) of the initial wave train. The wave train has become almost fully demodulated, as can be seen in the corresponding wave form.

This type of long-time behaviour of an unstable nonlinear system is unusual but not unknown. It was first discovered by Fermi, Pasta & Ulam (1940) during numerical
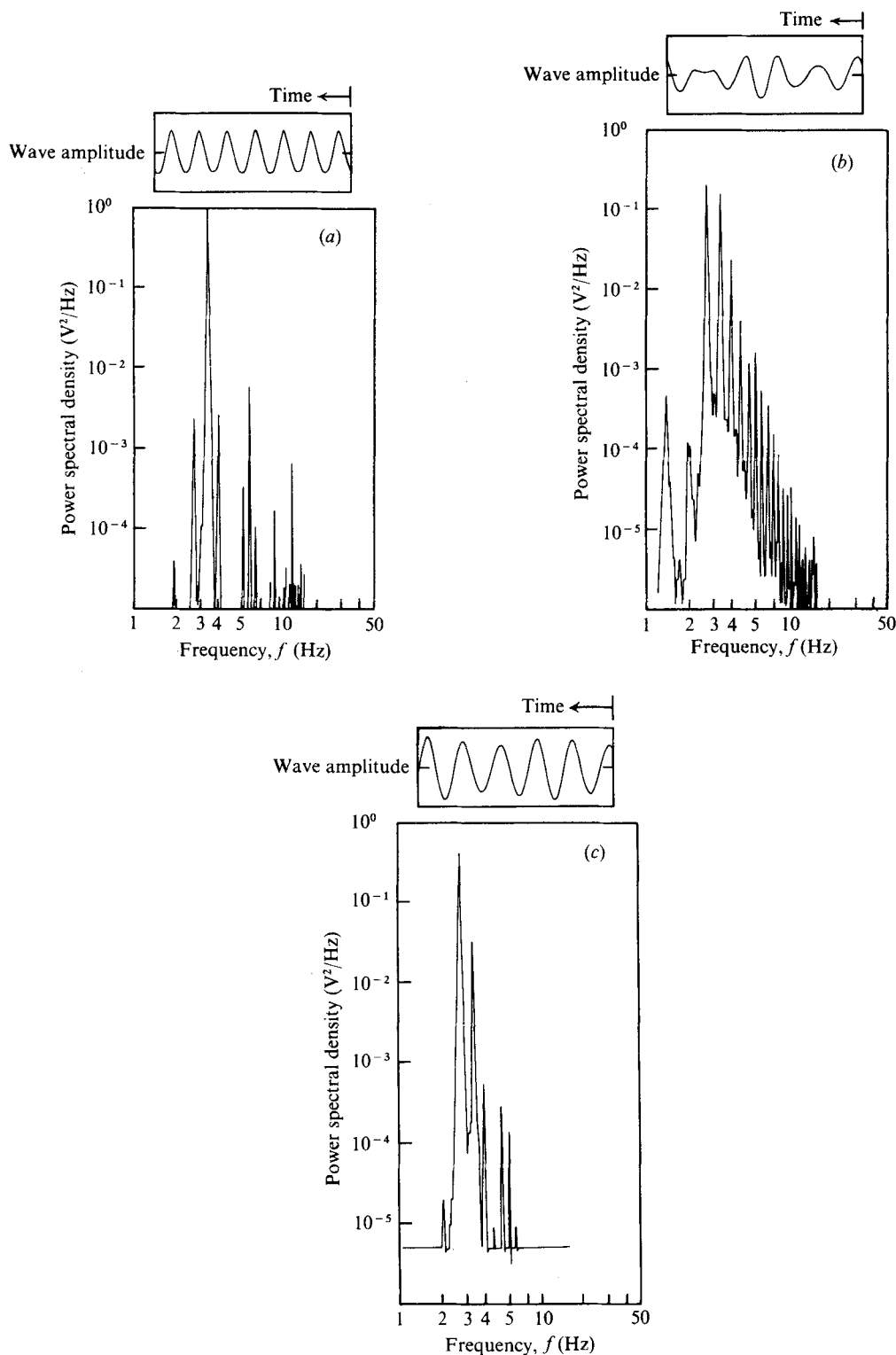
FIGURE 6. Evolution of a nonlinear finite amplitude wave train: wave forms and power spectral densities *vs.* propagation distance. (*a*) Initial stage of side-band growth, $x = 5$ ft, carrier wave with small amplitude modulation. (*b*) $x = 10$ ft, strong amplitude modulation, energy spread over many frequency components. (*c*) $x = 25$ ft, reduced amplitude modulation, return of energy to frequency components of original carrier wave, its side bands and harmonics. $f_0 = 3·25$ Hz, $(ka)_0 = \delta = 0·23$, $(ka)_{5\,ft} = 0·29$.

work on anharmonic lattice vibrations, and has become known as the Fermi–Pasta–Ulam, or FPU, recurrence phenomenon. Nonlinear systems which exhibit FPU recurrence are characterized by the general property that instabilities which lead to large modulations and a spread of energy over many spectral components do not ultimately lead to a complete thermalization of the energy and a random end state. Instead, the energy returns to the initial modes, and the initial wave form is reconstructed, or almost reconstructed, at the end of one cycle of modulation and demodulation. In the absence of additional effects such as dissipation, the end state of such systems is actually a continuing series of these recurrence cycles. We believe that our wave-train experiments strongly suggest that, in the absence of dissipative effects, the end state of the evolution of a nonlinear wave train on deep water is neither random nor steady, but is a series of periodically recurring states.

3.3. *Numerical computations and discussion*

For weakly nonlinear deep-water waves with a carrier frequency ω_0 (in radians, and hence a carrier wavenumber k_0), it was shown by Zakharov (1968), Hasimoto & Ono (1972) and Davey (1972) that the complex envelope $A = a e^{i\theta}$ obeys the nonlinear Schrödinger equation:

$$i \left(\frac{\partial A}{\partial t} + \frac{\omega_0}{2k_0} \frac{\partial A}{\partial x} \right) - \frac{\omega_0}{8k_0^2} \frac{\partial^2 A}{\partial x^2} - \tfrac{1}{2} \omega_0 k_0^2 |A|^2 A = 0. \tag{1}$$

The free-surface elevation η is related to A by

$$\eta = \mathrm{Re}\{A \exp[(i(k_0 x - \omega_0 t)]\}. \tag{2}$$

To obtain (1), it must be assumed that viscous effects are small, and that the wavenumber and frequency modulations, given by $\partial\theta/\partial x$ and $-\partial\theta/\partial t$, respectively, are small compared with the carrier wavenumber k_0 and frequency ω_0.

The initial-value problem for (1) has been solved exactly by Zakharov & Shabat (1972) for initial conditions which approach zero sufficiently rapidly as $|x| \to \infty$ (i.e. for envelope pulses), using the inverse scattering method. The exact solution predicts that an arbitrarily shaped initial envelope pulse will disintegrate into a definite number of solitons and an oscillatory tail. The tail is relatively small and unimportant, and it disperses linearly, resulting in a $t^{-\frac{1}{2}}$ amplitude decay. The solitons are permanent, progressive envelope pulses with sech profiles and heights that are inversely proportional to their characteristic widths. The solitons are stable in the sense that they can survive interactions with each other with no permanent change other than a possible shift in position and phase. These theoretical predictions of Zakharov & Shabat (1972) were later tested experimentally by Yuen & Lake (1975). Their measurements of wave-envelope pulses propagating in a deep-water wave tank provide good qualitative verification of the evolution and interaction properties predicted by the exact solutions of the nonlinear Schrödinger equation. They also compared the experimental measurements with results of numerical computations and found that the equation provides a good quantitative description of the evolution of nonlinear wave-envelope pulses on deep water.

For the case of the evolution of a nonlinear continuous wave train, the inverse scattering method does not apply and no exact analytical solution to the nonlinear Schrödinger equation has yet been found. As discussed by Benney & Newell (1967),

Zakharov (1968) and Hasimoto & Ono (1972), however, it can be shown that a stability analysis of the nonlinear uniform wave-train solution $A = a_0 \exp\left(-\frac{1}{2}ik_0^2 a^2 \omega_0 t\right)$ to the nonlinear Schrödinger equation recovers the results of the Benjamin & Feir stability analysis, which we have verified experimentally. In addition, the pulse experiments provide good evidence that (1) gives the correct asymptotic behaviour for wave-envelope pulses. We are therefore confident that a uniformly valid description of the evolution of a nonlinear continuous wave train can be obtained by solving an initial-value problem for (1). *For the problem of a continuous wave train the solution must be obtained numerically.*

We have developed a numerical program which solves initial-value problems for the nonlinear Schrödinger equation using a modified split-step Fourier method. The program solves the problem of the time evolution of a wave train that is periodic in x, with period equal to the length of the wave-train segment, and that is infinite in extent. In the laboratory, the wave train evolves as it propagates in the $\bar{x}$ direction from an initial state given at $\bar{x} = 0$ and is periodic in $\bar{t}$, where $(\bar{x}, \bar{t})$ are the physical coordinates. Thus the results of the numerical computations can be transformed to correspond to this situation by means of the co-ordinate transformation $(x, t) = (C_g \bar{t}, \bar{x}/C_g)$, where $C_g = \omega_0/2k_0$. We have used this transformation, which was also employed by Benjamin & Feir (1967), Benjamin (1967) and Chu & Mei (1970, 1971) in making comparisons between the results of theory and experiment.

The use of an initial-value problem for the evolution of a segment of a wave train with periodic boundary conditions to model the problem of the evolution of a continuous wave train is motivated, and we believe well justified, by our experimental measurements of wave-train evolution. We have found experimentally that the period of the modulation of a nonlinear wave train remains constant throughout the process of evolution, even while the wave train evolves through stages in which the modulation magnitude reaches a maximum and individual waves become so steep that small-scale wave breaking or generation of parasitic capillary waves occurs near their crests. The constancy of the modulation period of a wave train as it evolves from an initially unmodulated condition can be seen in the wave records of figure 1. The series of measured wave forms in figure 7 shows an example of the preservation of constant modulation period during the evolution of an initially strongly modulated wave train. For the case shown in figure 7, the modulation became so strong that the most-amplified waves in each modulation period experienced wave breaking or generation of capillary waves near the 12 ft station in the tank. The wave records in the figure show that the modulation passed through a pulse-train stage at about 15 ft. As it evolved further it demodulated somewhat, completing an FPU recurrence cycle at the 25 ft station, where there is a nearly exact reconstruction of the wave form measured at the 5 ft station. The examples in figures 1 and 7 are typical of our experimental results in that, throughout the entire process of wave-train evolution, the period of the modulation remains unchanged. Since the period of the modulation is constant, the evolution of the wave train can be computed by solving the nonlinear Schrödinger equation for the evolution of a segment of the wave train having the length of one modulation period with periodic boundary conditions. For problems involving initially unmodulated wave trains the computations can be performed using a very small initial modulation magnitude, and the appropriate modulation length may be obtained from the initial condi-
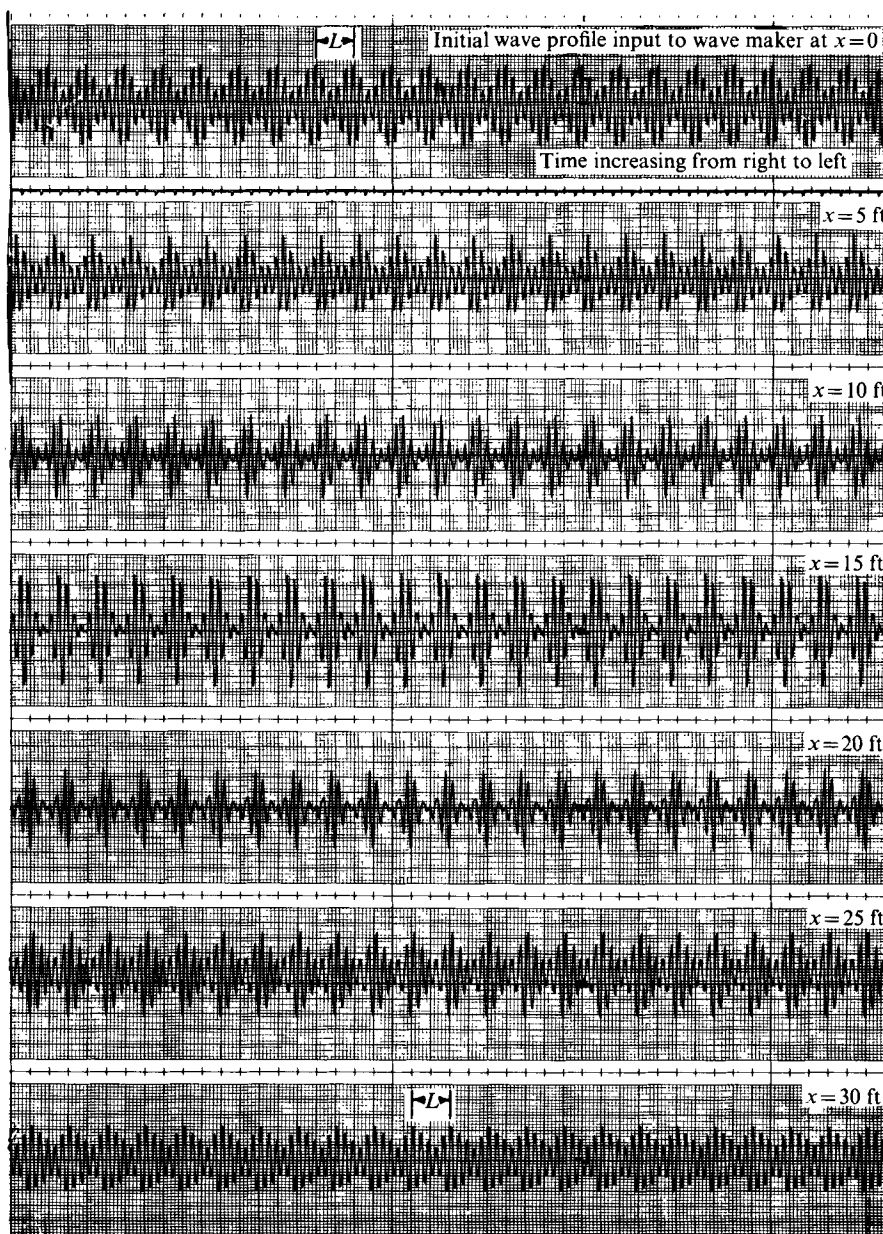
FIGURE 7. Typical wave amplitude records of the evolution of a wave train with large initial modulation. Initial conditions: $\delta = 0.2$, $(ka)_0 \simeq 0.2$, $S_0 \simeq 0.5$, $f_0 = 2.5$ Hz. Notice that the period of the modulation (denoted by L) remains unchanged even though the waves themselves undergo strong modulation with wave breaking and capillary generation occurring near $x = 12$ ft.

tions using the condition for the most unstable initial modulation as given by the stability analysis.

Furthermore, the constancy of the modulation period during the evolution of a nonlinear wave train, together with the known properties of nonlinear wave-envelope pulses, suggests the following phenomenological interpretation of wave-train evolution

3

and FPU recurrence in terms of solitons and tails. If the evolution of a single modulation period of a wave train is treated as though it were an isolated pulse, one knows from the exact solutions for pulses that it will evolve into a fixed number of solitons and a tail. Since the pulse is actually a segment of a wave train that has periodic modulations, however, it has neighbours which evolve in the same manner as it does and so it is subject to periodic boundary conditions. As the pulse and its neighbours evolve in the process of soliton formation, their soliton components change alignment. This alters the wave-form modulations and produces a spread of energy over many components in the spectrum. If the soliton components have speed differences, the components which leave on one side of a modulation period are replaced by their counterparts from the pulse on the other side. Because of the stability of the solitons and their formation process, the only effect of the interactions is a series of phase shifts, so that the soliton components will eventually return to their original alignment and reconstruct the initial state of the wave train, except for imperfections which arise owing to the effects of dissipation and the small contribution of the dispersive tails. A similar argument was first offered as an explanation of FPU recurrence by Zabusky & Kruskal (1965), who observed recurrence phenomena in numerical solutions of the Korteweg–de Vries equation. At the time of their investigation exact solutions of the equation had not yet been found and consequently the existence of the tail and its role were not identified.

If two or more soliton components have no net difference in speed, the above argument must be modified. Recurrence is still possible, however, because, as shown by Roskes (1976), interactions between soliton components propagating at the same speed can produce a series of shifts in relative phase or position which will lead eventually to recurrence in the evolution of a true pulse initial condition. It follows, therefore, that the same process should also lead to recurrence in nonlinear wave trains when there are no speed differences between the soliton components of each modulation period. In fact, it is interesting to note here that the recurrence times we have observed in our wave-train experiments are of approximately the same length as the times required for the emergence of soliton components in our earlier pulse experiments, and that the soliton components of each pulse had at most only very small speed differences. For this reason we suspect that the recurrence we have observed in our wave-train experiments is best described in terms of interactions between solitons which have no net speed differences.

The results of our numerical computations of wave-train evolution demonstrate that solutions to initial-value problems for the nonlinear Schrödinger equation with periodic boundary conditions exhibit FPU recurrence. In the absence of dissipative effects, the recurrence leads to a perfect reconstruction of the initial conditions. An example of the computed time evolution of the envelope of a modulated wave train is shown in figure 8. The initial envelope was given a 10 % modulation at the wavelength corresponding to the most unstable Benjamin–Feir modulation for the wave train, and the results shown in the figure extend over one modulation period in space. The modulation of the computed wave envelope grows in time, reaches a maximum at time = 5·3 and returns to the initial level, completing one FPU recurrence cycle, at time = 31·8,

For comparison with experimental data, we have also transformed the results of such numerical calculations to obtain power spectra at various stages of wave-train evolution. When this is done, the magnitudes of the pair of side-band frequency components which characterize the amplitude modulation can be evaluated and normalized using the magnitude of the carrier frequency component. An example of such a com-
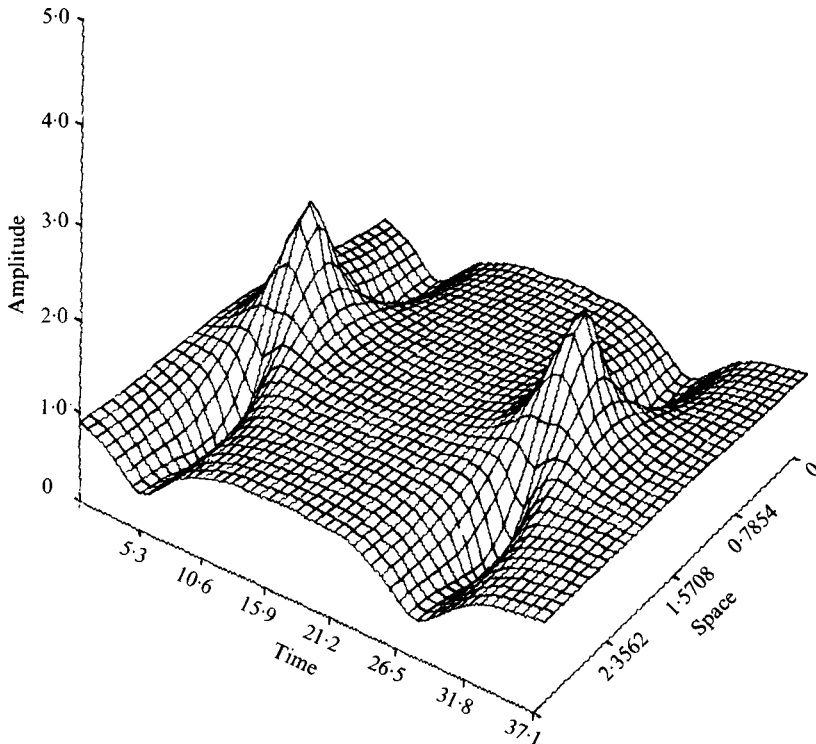
FIGURE 8. Fermi–Pasta–Ulam recurrence in nonlinear Schrödinger equation. The amplitude of the solution of the nonlinear Schrödinger equation is plotted against non-dimensionalized space ($\frac{1}{2}k\zeta$) and time ($\frac{1}{2}\omega_0 k_0^2 a_0^2 t$). Initial condition contains a 10 % sinusoidal modulation which corresponds to the most unstable Benjamin–Feir perturbation. It can be seen that the maximum modulation is attained at time = 5·3; the time required for a complete recurrence cycle is time = 31·8.

parison is shown in figure 9, where the measured and calculated results for the evolution of a nonlinear wave train are compared using the average normalized energy of the side-band frequency components. The experimental data were obtained from a series of measurements of the type shown in figure 3, for which several different initial modulation magnitudes were imposed in order to obtain measurements of wave-train evolution over an effective propagation distance longer than the length of the wave tank. The theoretical curves in figure 9 include the result from the Benjamin–Feir linearized stability analysis, the result from the inviscid solution of the nonlinear Schrödinger equation and results from solutions of the nonlinear Schrödinger equation with an additional term used to model the effects of dissipation. Each has been matched in magnitude to the side-band energy level measured at a propagation distance of 5 ft and calculated using the effective initial value of $(ka)_0$ determined from the amplitude and frequency measured at the 5 ft station as described in §3.1.

The dash–dot curve in the figure is a result of the inviscid calculation using the non-linear Schrödinger equation with no dissipative effects included. At the initial stage of evolution, it can be seen that this result is in agreement with the growth rate predicted by Benjamin & Feir (given by the dashed curve) as well as with the experimental data. The Benjamin & Feir result, however, corresponds to unbounded growth of the dis-
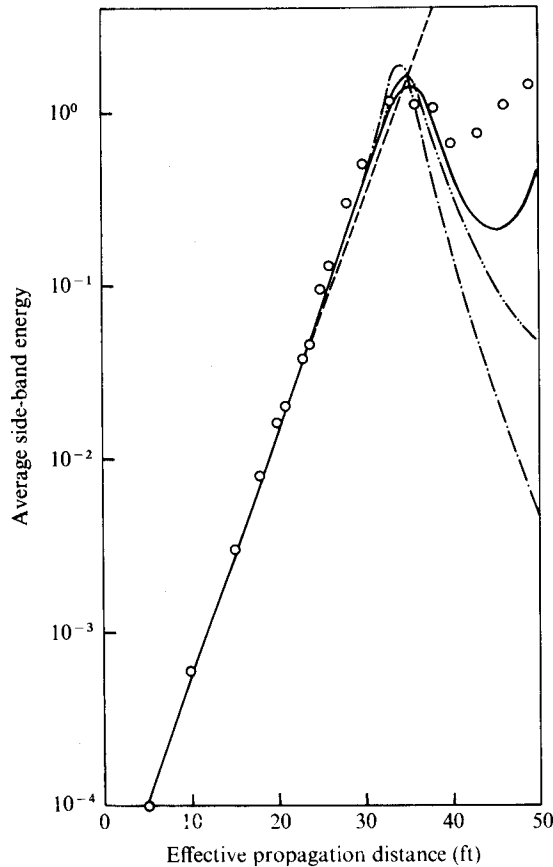
FIGURE 9. Comparison of numerical and experimental results for the evolution of a wave train from nearly uniform initial conditions, as measured by the normalized average energy of the most unstable Benjamin–Feir side-band components. The numerical solutions show the effect of including dissipation and wave breaking in the calculations. ○, experiment, $(ka)_0 = 0\cdot16$; ———, Benjamin & Feir (1967); —·—, nonlinear theory, inviscid; —··—, nonlinear theory with dissipation; ——, nonlinear theory with dissipation plus wave breaking.

turbance, whereas the results from the Schrödinger equation and the experimental data indicate that the magnitudes of the side-band ratios reach a saturation level and eventually subside, reflecting the tendency of the wave train to demodulate and undergo recurrence. We feel that it is important to note that, even when dissipation is neglected in the calculations, the time at which the saturation occurs as calculated using the nonlinear Schrödinger equation is in good agreement with the time of occurrence of side-band saturation in the experimental data.

Beyond this stage of evolution, however, a substantial difference develops between the results of the inviscid theory and the results of the experiments. The cause of this discrepancy appears to be attributable to the fact that dissipation has been neglected in the calculations. The inviscid solution of the nonlinear Schrödinger equation predicts demodulation at an exponential rate and eventual reconstruction of the initial conditions on the completion of one FPU cycle. The data show a much smaller reduction in side-band energy, followed by renewed growth of the average side-band energy

levels. Although representation of the wave-train properties in terms of the normalized average side-band energy should effectively scale out the first-order (linear) effects of dissipation, there can be secondary (nonlinear) effects which are not scaled out by the normalization and which may become significant during the long-time evolution of the wave train. One such effect is an alteration of the time scale or rate of evolution. In order to investigate the importance of such dissipative effects on the characteristics of the long-time evolution of nonlinear wave trains, we have performed calculations using the nonlinear Schrödinger equation with an additional term to model dissipation:

$$i\left(\frac{\partial A}{\partial t}+\frac{\omega_0}{2k_0}\frac{\partial A}{\partial x}+\nu A\right)-\frac{\omega_0}{8k_0^2}\frac{\partial^2 A}{\partial x^2}-\tfrac{1}{2}\omega_0 k_0^2 |A|^2 A = 0. \tag{3}$$

When ν is a constant, the added term introduces a constant exponential decay in the case of infinitesimal waves, and is a generally accepted model for the viscous dissipation of surface waves. Computations using values of ν typical of that of the kinematic viscosity of water yield results which exhibit a trend towards agreement with the data, but still fall short of actual agreement. An example of such a calculation is shown in figure 9.

We recall, however, the fact that in the experiments formation of capillary waves and wave breaking often occurred when the wave trains were strongly modulated. Both of these activities are extremely effective in dissipating wave energy. It therefore appears that abnormally large dissipative effects may be present when the wave trains are strongly modulated. To model this type of abruptly increasing dissipation, we have allowed the value of ν to be a function of time. Specifically, we have allowed ν to take the usual value based on the kinematic viscosity of water as long as the steepness of the wave train remains small everywhere, but have let it increase exponentially with increasing wave steepness once the local steepness of the wave train exceeds the value beyond which capillary waves were observed in the experiments. Furthermore, in view of the fact that the measured gravity waves never had a value of ka in excess of the Stokes limiting value of 0·448, we have constructed the dissipation model such that the dissipation becomes infinitely large as the Stokes value is approached. The resulting expression for ν is

$$\nu = \nu_1 \exp\left\{\mu\frac{(ka)_m - (ka)_{\mathrm{cap}}}{(ka)_s - (ka)_m}\right\} H[(ka)_m - (ka)_{\mathrm{cap}}], \tag{4}$$

where $(ka)_m$ is the maximum steepness in a modulation period at a fixed time step, $(ka)_{\mathrm{cap}}$ is the minimum steepness at which formation of capillary waves is first observed (estimated to be approximately equal to 0·3 on the basis of experimental observations) and $(ka)_s = 0\cdot448$ is the Stokes limiting steepness. The quantities ν_1 and μ are adjustable parameters. An example of the results of calculations using this dissipation model and relatively conservative estimates of ν_1 and μ is shown in figure 9. The results of the calculations performed using this dissipative model are in much better agreement with the experimental data than are the results of the non-dissipative calculations. Although the dissipation model we have used to explore the consequences of a large and abrupt dissipative mechanism is admittedly both crude and arbitrary, the extent to which it improves the agreement between the experimental and numerical results indicates to us that in cases where we have observed significant differences between the measured and predicted long-time characteristics of nonlinear wave trains, as in figure 9, the

differences can be attributed to the long-time effects of dissipation. This appears to be true for differences in the extent of recurrence, for example, but it is interesting to note once more that the point at which the wave-train modulations reach their maximum level, and demodulation begins, is well predicted by both the inviscid and the dissipative version of the Schrödinger equation. It should also be pointed out that, once nonlinear wave trains have become highly modulated, a representation of wave-train evolution which is based on the behaviour of only three modes (two side bands normalized by the primary, as in figure 9) is not complete, and does not bring out the features of FPU recurrence nearly as strongly as do either the original wave records or the full spectra.

Comparisons of the experimental measurements and the results of numerical solutions of the nonlinear Schrödinger equation indicate that there is good qualitative agreement between the observed behaviour of nonlinear wave trains and the phenomena predicted using the equation. Furthermore, the experimental and numerical results agree quantitatively for the early stages of wave-train evolution and for long-time evolution as well, if an appropriate model is used to account for the long-time effects of dissipation (additional comparisons are reported in Lake *et al.* 1976). The comparisons indicate that this is true even when wave trains become so strongly modulated that, at isolated locations, individual waves become steep enough to generate capillary waves or even to break. These violent but localized activities appear to have little effect on wave-train evolution other than to cause an enhancement of dissipation. When the added dissipation is taken into account, the system is still well described by the nonlinear Schrödinger equation. This seems somewhat surprising since the theory is a weakly nonlinear theory, and one expects it to be inapplicable when waves are so steep that they break. On the other hand, it can be argued that the mismatch in scales between these events and the envelope modulation is so great that direct interaction is highly unlikely, and the net effect of enhanced dissipation is really a reasonable consequence. One still has to marvel at the wide range of applicability of the nonlinear Schrödinger equation, which is a result of retaining only the first nonlinear term in the Stokes expansion. The following observation may be interesting. It is widely accepted that the Stokes limit ($ka = 0.4488$) gives a theoretical upper bound for the ka of a gravity wave. Experimental evidence has more or less borne out this assertion; ka as measured by a wave gauge rarely, if ever, exceeds 0.38. This means that, even at the point of wave breaking, the magnitude of this nonlinear correction in the dispersion relation, which is responsible for the form of (1), still does not exceed 10% of that of the linear term. Strictly speaking, since we have not estimated the possible contribution of other terms in the series, this cannot be used as an explanation for the success of the nonlinear Schrödinger equation. However, we can consider this as being suggestive of the possibility that, as far as the envelope evolution is concerned, gravity waves are weakly nonlinear in nature. The detailed processes of wave breaking and related phenomena are, of course, not described by the weakly nonlinear theory.

There is one characteristic of the long-time evolution of nonlinear wave trains which we have observed in many of our experiments but which cannot be found in numerical solutions of the nonlinear Schrödinger equation (either inviscid or dissipative). When experiments were performed using initially uniform, or nearly uniform, wave trains with large initial steepness, recurrence cycles were observed in which the wave trains became strongly modulated and then demodulated until they were again nearly uni-

form. In these cases, however, as the wave trains demodulated and the energy returned to the frequency components of the original wave trains (carrier, side bands and harmonics), the lower side-band component became much stronger than the upper side-band component and eventually became stronger than the component at the carrier frequency. As the wave trains became uniform again, the wave forms and the power spectra clearly showed that the dominant component was the component at the frequency of the lower side band of the original carrier. This phenomenon is evident in the wave forms and spectra of figures 5 and 6. It is recurrence in the sense that the wave trains become uniform and their wave energy returns to the components of their initial spectra, but the uniform wave trains which reappear are not exact reconstructions of the originals because they have new, lower, carrier frequencies. This dominance of the lower side-band component cannot occur in numerical solutions of the nonlinear Schrödinger equation, as can be seen by noting that during the initial stages of evolution of such wave trains the side-band components are symmetric about the carrier frequency, and that this initial symmetry will be preserved in the solutions of the equation throughout the entire FPU recurrence process. Although we do not have a good explanation for the shift to lower carrier frequencies that we have observed in these experiments, there is some evidence that it may be associated with the fact that the steepness of gravity waves cannot increase beyond a fixed limiting value. In experiments where wave trains were generated with strong initial modulations and large initial steepness, we have observed that recurrence cycles occur without changes in the wave-train carrier frequency. An example of such a case is shown in figure 7. The significant difference between these cases and the cases for which there are carrier-frequency changes appears to be the amount by which the steepness of the most amplified waves in the modulations of the evolving wave trains ultimately increases over the steepness of the initial waves. If the initial steepness of the waves in a uniform wave train and the initial steepness of the largest wave in a strongly modulated wave train are of the same magnitude and are large, the most amplified waves which occur during the evolution of the initially uniform wave train will be much steeper than any of the waves which develop during the evolution of the initially modulated wave train. This observation suggests to us that the shift to a lower carrier frequency, and therefore to a longer length scale and lower wave steepness, may take effect when wave-train modulations would otherwise require that individual waves exceed the maximum realizable wave steepness. The fact that there were waves which were modulated to the point of capillary generation or breaking in every case where a carrier-frequency change was measured is consistent with this hypothesis. Another possibility is that the dominance of the lower side band is caused by dissipation. Since the effects of dissipation would tend to favour the survival of the lower modes over the higher, the qualitative trend would be correct. It seems somewhat unlikely, however, that dissipative effects alone could account for the relatively rapid development of very pronounced differences in the magnitude of components which have such small frequency differences as do the side-band and carrier components of these wave trains. Although we are unable at this time to offer a satisfactory explanation of this phenomenon, we believe that it is a potentially important characteristic of evolving nonlinear wave trains and one that is worthy of further investigation.

4. Conclusions

Experiments have been performed to investigate the evolution of a nonlinear continuous wave train on deep water. During the initial stage of evolution, amplitude modulations develop and grow exponentially as predicted by the stability analysis of Benjamin & Feir (1967). When the magnitude of the modulations, measured by the ratio of the energy in the growing side-band frequency components normalized by the energy in the carrier frequency component, becomes of order 10^{-1} the results of the stability analysis no longer apply. The further evolution of the wave train is characterized by continued growth of the modulations accompanied by a spread of energy over many spectral components, and then demodulation and return of the energy to the original spectral components of the initial wave train. The experimental results strongly suggest that the end state of the evolution of a nonlinear wave train, in the absence of dissipative effects, would be a continuing series of modulation–demodulation FPU recurrence cycles. The measurements also show that the period of the modulations remains constant during the process of evolution. For an initially uniform wave train in the presence of random infinitesimal perturbations, the modulation period can be determined from the initial conditions using the results of the stability analysis of Benjamin & Feir (1967). Results of previous investigations have shown that the governing equation for nonlinear deep-water waves with a carrier frequency is the nonlinear Schrödinger equation (Zakharov 1968), that the equation reproduces the Benjamin–Feir stability results (Benney & Newell 1967; Zakharov 1968), and that the equation provides a quantitatively correct description of the long-time evolution of nonlinear wave pulses (Yuen & Lake 1975). The equation should therefore provide a uniformly valid description of the evolution of a nonlinear continuous wave train. The existence of a known and constant modulation period makes it possible to obtain numerical solutions of the nonlinear Schrödinger equation for the evolution of a nonlinear continuous wave train by solving for the evolution of one modulation period of the wave train subject to periodic boundary conditions. The results of these numerical solutions of the nonlinear Schrödinger equation have been found to exhibit the FPU recurrence phenomenon, confirming the indications of the experiments regarding the long-time behaviour of nonlinear wave trains. The constancy of the period of wave-train modulations, and the known properties of evolving nonlinear wave pulses and solitons have been used to provide a phenomenological description of the FPU recurrence process. Comparisons of the experimental data with results from numerical solutions of the nonlinear Schrödinger equation show that the equation provides a good quantitative description of wave-train evolution from the earliest stage of instability through the stages where the modulations become very strong, reach a maximum and then begin to subside. At still later stages, the experimental and numerical results are in qualitative agreement on the tendency of the wave trains to return to uniform conditions and undergo continued recurrence cycles. Comparisons between the measured data and numerical solutions of the equation with terms added to model dissipative effects indicate that the observed quantitative differences between experiment and theory at the later stages of evolution may be attributed to the long-time effects of dissipation, which eventually become significant in the experiments. Under certain conditions, the evolving wave trains exhibit a shift to a new, lower, effective carrier frequency as they undergo strong modulations and return to uniform

conditions. This phenomenon is not predicted by solutions of the nonlinear Schrödinger equation and may be associated with amplification of individual waves to their maximum realizable values of steepness, although no satisfactory explanation for the phenomenon has yet been found.

The results of this investigation provide evidence that the end state of the evolution of a non-dissipative nonlinear continuous wave train is neither steady nor random, but is instead a series of periodically recurring states. The nonlinear resonant interactions which occur during the evolution of a nonlinear wave train on deep water do not lead to an irreversible spread of energy over all spectral components; in fact, coherence is retained throughout the process of evolution. In realistic environments coherence will be lost ultimately not as a result of the nonlinearity of the wave trains but because of the long-time effects of dissipative mechanisms such as surface viscous dissipation, generation of capillary waves and wave breaking.

REFERENCES

BENJAMIN, T. B. 1967 Instability of periodic wavetrains in nonlinear dispersive systems. *Proc. Roy. Soc.* A **299**, 59.

BENJAMIN, T. B. & FEIR, J. E. 1967 The disintegration of wave trains in deep water. Part 1. Theory. *J. Fluid Mech.* **27**, 417.

BENNEY, D. J. & NEWELL, A. C. 1967 The propagation of nonlinear wave envelopes. *J. Math. Phys.* **46**, 133.

CHU, V. H. & MEI, C. C. 1970 On slowly-varying Stokes waves. *J. Fluid Mech.* **41**, 873.

CHU, V. H. & MEI, C. C. 1971 The nonlinear evolution of Stokes waves in deep water. *J. Fluid Mech.* **47**, 337.

DAVEY, A. 1972 The propagation of a weak nonlinear wave. *J. Fluid Mech.* **53**, 769.

FEIR, J. E. 1967 Discussion: some results from wave pulse experiments. *Proc. Roy. Soc.* A **299**, 54.

FERGUSON, W. E. & YUEN, H. C. 1977 Evolution of a nonlinear wavetrain in two space dimensions. To appear.

FERMI, E., PASTA, J. & ULAM, S. 1940 Studies of nonlinear problems. In *Collected Papers of Enrico Fermi*, vol. 2, p. 978. University of Chicago Press, 1962.

HASIMOTO, H. & ONO, H. 1972 Nonlinear modulation of gravity waves. *J. Phys. Soc. Japan* **33**, 805.

HASSELMANN, K. 1963 On the nonlinear energy transfer in a gravity-wave spectrum. Part 2. Conservation theorems; wave-particle analogy; irreversibility. *J. Fluid Mech.* **15**, 273.

HASSELMANN, K. 1967 Discussion. *Proc. Roy. Soc.* A **299**, 76.

LAKE, B. M. & YUEN, H. C. 1976 A new model for nonlinear wind-waves. *TRW Rep.* no. 26062-6014-RU-00. (See also *Proc. Conf. Geofluiddyn. Wave Math., Seattle*, 1977, to appear.)

LAKE, B. M. & YUEN, H. C. 1977 A note on some nonlinear water-wave experiments and the comparison of data with theory. *J. Fluid Mech.* **83**, 75.

LAKE, B. M., YUEN, H. C., RUNGALDIER, H. & FERGUSON, W. E. 1976 Nonlinear deep water waves: theory and experiment. II. Evolution of a continuous wavetrain. *TRW Rep.* no. 26062-6012-RU-00.

LEWIS, J. E., LAKE, B. M. & KO, D. R. S. 1974 On the interaction of internal waves and surface gravity waves. *J. Fluid Mech.* **63**, 773.

LIGHTHILL, M. J. 1965 Contributions to the theory of waves in nonlinear dispersive systems. *J. Inst. Math. Appl.* **1**, 269.

LIGHTHILL, M. J. 1967 Some special cases treated by the Whitham theory. *Proc. Roy. Soc.* A **299**, 28.

ROSKES, G. 1976 Comments on 'Nonlinear deep water waves: theory and experiment' by H. C. Yuen and B. M. Lake. *Phys. Fluids* **19**, 766.

WHITHAM, G. B. 1965 A general approach to linear and non-linear dispersive waves using a Lagrangian. *J. Fluid Mech.* **22**, 273.

YUEN, H. C. & LAKE, B. M. 1975 Nonlinear deep water waves: theory and experiment. *Phys. Fluids* **18**, 956.

ZABUSKY, N. J. & KRUSKAL, M. D. 1965 Interaction of 'solitons' in a collisionless plasma and the recurrence of initial states. *Phys. Rev. Lett.* **15**, 240.

ZAKHAROV, V. E. 1968 Stability of periodic waves of finite amplitude on the surface of a deep fluid. *Sov. Phys. J. Appl. Mech. Tech. Phys.* **4**, 86.

ZAKHAROV, V. E. & SHABAT, A. B. 1972 Exact theory of two-dimensional self-focusing and one-dimensional self-modulating waves in nonlinear media. *Sov. Phys. J. Exp. Theor. Phys.* **34**, 62.